World Academy of Science, Engineering and Technology
International Journal of Civil and Environmental Engineering
Vol:10, No:12, 2016

Constitutive Modeling of Different Types of Concrete under Uniaxial Compression

Mostafa Jafarian Abyaneh, Khashayar Jafari, Vahab Toufigh

***Abstract*—**The cost of experiments on different types of concrete has raised the demand for prediction of their behavior with numerical analysis. In this research, an advanced numerical model has been presented to predict the complete elastic-plastic behavior of polymer concrete (PC), high-strength concrete (HSC), high performance concrete (HPC) along with different steel fiber contents under uniaxial compression. The accuracy of the numerical response was satisfactory as compared to other conventional simple models such as Mohr-Coulomb and Drucker-Prager. In order to predict the complete elastic-plastic behavior of specimens including softening behavior, disturbed state concept (DSC) was implemented by nonlinear finite element analysis (NFEA) and hierarchical single surface (HISS) failure criterion, which is a failure surface without any singularity.

***Keywords*—**Disturbed state concept, hierarchical single surface, failure criterion, high performance concrete, high-strength concrete, nonlinear finite element analysis, polymer concrete, steel fibers, uniaxial compression test.

I. Introduction

FROM ancient history of civil engineering, the idea of combining two or more different materials resulting in a new composite material with improved properties has fascinated humankind life. Concrete is a composite material made of coarse and fine aggregates bonded together with a time-based hardening adhesive. In this century, extensive and growing applications of concrete in structures have raised a great attention toward investigation and prediction of concrete behavior. The great advantages of concrete are availability, relatively low cost, durability, stability against temperature changes, and capability of being poured into molds with different shapes.

Polymerization of a monomer-aggregate mixture leads to a special type of concrete, namely PC, which was introduced in late 1950's and become well-known in 1970's [1]. Cementitious material of PC is epoxy resin as opposed to cement and water of cement concrete. Changing the type and proportion of concrete components could result in a new concrete behavior with desirable strength, density, and resistance to environmental attacks. Superior properties of PC include high compressive strength and strain, durability, fast curing, resistance to chemical attack, and excellent bond to cement concrete and steel reinforcement. Due to these special characteristics, PC has been extensively used as a repairing material [2].

M. Jafarian Abyaneh, K. Jafari, and V. Toufigh (Assistant professor) are with Department of Civil Engineering, Sharif University of Technology, Azadi st, Tehran, Iran (e-mail: mjafarianabyaneh@gmail.com, khashijafari71@yahoo.com, toufigh@sharif.edu).

In the literature, there are several studies on normal, high-strength, and lightweight cement concrete that address their mechanical behavior under uniaxial compression test. Wee et al. [3] experimentally and analytically studied the behavior of normal concrete under uniaxial compression by changing the water-to-cement ratio, admixture type, and the age at which experiments were conducted. Lim and Ozbakkalogu [4] statistically modeled normal, lightweight, and HSC behavior under different testing conditions including uniaxial compression based on the available experimental database. Nevertheless, the aforementioned model lacks any physical meaning for applying to other types of concrete including PC.

Farnam et al. [5] and Noori et al. [6] studied and modeled the behavior of HPC and HSC, respectively, in uniaxial loading by using Mohr-Coulomb and William-Warkane failure criteria. Toufigh et al. [7] investigated the behavior of PC under uniaxial compression test by using DSC and HISS plasticity model. However, there are few researches in the literature that provide a complete constitutive model for behavior of different types of concrete, particularly PC. The complete elastic-plastic behavior of concrete is mainly based on axial plastic strain, similar to other brittle materials such as rock and soil. Thus, there is an increasing demand for predicting mechanical behavior of PC under compression through its axial strain.

In this research, a wide range of data sets for different types of concrete specimens under uniaxial compression from previous researches have been numerically modeled. These types of concrete include HSC, HPC, and PC. It is worth noting that an advanced numerical model predicting the complete behavior of concrete was developed using NFEA. The elastic-plastic response was modeled based on combination of HISS failure criterion and DSC.

II. Modeling

An advanced numerical model based on DSC and HISS failure criterion was developed to predict stress-strain behavior of different types of concretes considering its softening behavior under uniaxial compression loading. As mentioned before, several types of concrete from previous researches were modeled to show the extent of model's applicable materials.

A. DSC

The fundamental idea behind the applied model is based on DSC, which can be formulated as decomposition of material behavior into its relatively intact (RI) and fully adjusted (FA) components. A schematic illustration of DSC has been shown in Fig. 1. As can be seen in the figure, the blank and solid areas represent RI and FA parts, respectively. The initial response of material is absolutely RI without any visible cracks. As applied displacement increases, the FA response becomes more predominant with propagation of cracks resulting in completely FA behavior at the failure of corresponding specimen. Based on the concept proposed by Desai [8], the disturbance can be defined as:

$$D = D_u(1 - e^{-A\zeta_D^Z}) \tag{1}$$

where D_u is the ultimate value of disturbance; A and Z are material parameters; and ζ_D is the trajectory of deviatoric plastic strain as follows:

$$\zeta_D = \int (d\mathbf{E}_{ij}^p d\mathbf{E}_{ij}^p)^{\frac{1}{2}} \tag{2}$$

in which E_{ij} represents the deviatoric strain tensor of total strain tensor ε_{ij}. The disturbance of stress-strain curve can be generally expressed as:

$$D = \frac{\sigma^{RI} - \sigma^{obs}}{\sigma^{RI} - \sigma^{FA}} \tag{3}$$

where σ^{RI}, σ^{FA}, σ^{obs} are RI, FA, and observed stresses, respectively. In the presented model, this definition was also used for volumetric strain versus strain curve. In order to find A and Z parameters, (1) and (3) were equated for two arbitrary points of experimental curve. The disturbance parameters (A, Z, and D_u) were used for predicting experimental behavior of independent tests of the same material. The dependence of RI and FA states is different in the modeling procedure. The modulus of elasticity and the type of epoxy resin affect the RI behavior, while the confining conditions and residual strength control the FA behavior. After determination of disturbance parameters for each specimen, stress increments can be obtained by using [8]:

$$d\sigma_{ij} = (1-D)C_{ijkl}^{ep} d\varepsilon_{kl} + \frac{D}{3}\delta_{ij}C_{ppkl}^{ep} d\varepsilon_{kl} - dD(\sigma_{ij}^{RI} - \sigma_{ij}^{FA}) \tag{4}$$

In the pre-failure stage where $D = 0$, Eq. (4) represents RI state. The RI response can be predicted by using different models from simple mathematical models to advanced models such as the HISS plasticity model. In this study, NFEA and HISS δ_0 plasticity model have been utilized in order to predict the RI response.

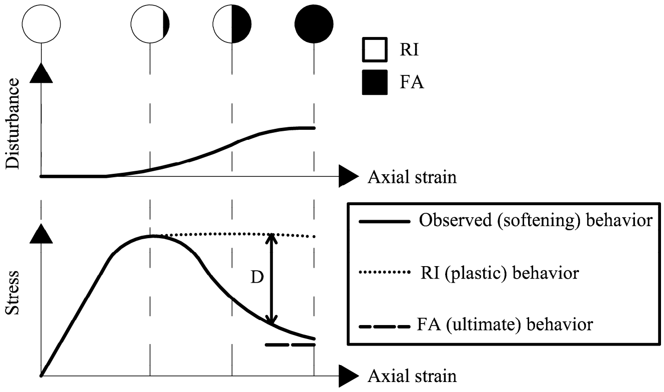

Fig. 1 Schematic representation of DSC decomposition

B. HISS Failure Criterion

A failure surface can be expressed as the boundary of elastic behavior and is usually written by means of stresses. Common simple failure criteria that have been employed in the literature are Tresca, Von-Mises, Mohr-Coulomb, and Drucker-Prager. Most of the plasticity models formulated for concrete consist of two surfaces resulting in singularity. The HISS failure criterion is an advanced model without any singularity, which means that it has no singularity point, leading to a more convenient yield surface in comparison to other conventional models. The aforementioned model can be adopted for materials with both isotropic and anisotropic hardening response as well as associated or non-associated plasticity characterizations, in order to predict the material response by means of the continuum plasticity theory. The yield function of HISS δ_0 plasticity model, which provides a general formulation for elastic-plastic behavior of materials is [9]:

$$f = \bar{J}_{2D} - (-\alpha\bar{J}_1^n + \gamma\bar{J}_1^2)(1-\beta S_r)^m = 0 \tag{5}$$

where $\bar{J}_{2D} = J_{2D}/p_a^2$; p_a is the atmospheric pressure constant; $\bar{J}_1 = (J_1 + 3R)/p_a$; R = the bonding stress; n = phase change parameters where the volume change transits from compaction to dilation or vanishes; $m = -0.5$ is often used; γ parameter related to the (ultimate) yield surface; β corresponds to the shape of yield function in the σ_1- σ_2- σ_3 space; S_r = stress ratio = $(\sqrt{27}/2).(J_{3D}/J_{2D}^{3/2})$; α is the hardening parameter which can be expressed in terms of deviatoric plastic strain trajectory; J_1 = the first invariant of stress tensor; and J_{2D} = the second invariant of deviatoric stress tensor.

C. NFEA

Since the applied load and geometry of specimens are axisymmetric, all quantities of interest in structural analysis including displacements, strains, and stresses are independent of the circumferential coordinate. Therefore, a plane whose width and length are radius and height of cylindrical specimen was modeled instead of modeling the whole specimen. For implementation of NFEA, a schematic plane shown in Fig. 2 was divided by a mesh containing 15 columns and 60 rows leading to 900 elements. In order to satisfy the equilibrium conditions between internal and external forces, the norm of following residual stress ($\boldsymbol{\psi}$) must approach zero through required iterations [10]:

$$\boldsymbol{\psi} = \int_{V} \bar{\mathbf{B}}\boldsymbol{\sigma} d_V - \mathbf{F} \tag{6}$$

where V is the volume of the specimen, $\mathbf{F}$ represents external forces tensor, $\boldsymbol{\sigma}$ is the Cauchy stress tensor, and $\bar{\mathbf{B}}$ is the tensor relating the increments of strain and displacement ($\Delta\boldsymbol{\varepsilon} = \bar{\mathbf{B}}\Delta\bar{\mathbf{u}}$). In order to find the value of stress in each step of loading, the increment of stresses can be expressed as:

$$\begin{Bmatrix} \Delta\boldsymbol{\sigma}_r \\ \Delta\boldsymbol{\sigma}_\theta \\ \Delta\boldsymbol{\sigma}_z \\ \Delta\boldsymbol{\sigma}_{rz} \end{Bmatrix} = \mathbf{C} \begin{Bmatrix} \Delta\boldsymbol{\varepsilon}_r \\ \Delta\boldsymbol{\varepsilon}_\theta \\ \Delta\boldsymbol{\varepsilon}_z \\ \Delta\boldsymbol{\gamma}_{rz} \end{Bmatrix} \tag{7}$$

in which $\mathbf{C}$ is the stiffness matrix, which can be elastic ($\mathbf{C}_e$) or elastic-plastic ($\mathbf{C}_{ep}$) depending on whether the corresponding Gaussian point has yielded or not. The indices r, θ, and z represent radial, angular, altitudinal components of stress and strain. Elastic-plastic stiffness matrix can be expressed as:

$$\mathbf{C}_{ep} = \mathbf{C}_e - \frac{\mathbf{C}_e \mathbf{n}\mathbf{n}^T \mathbf{C}_e}{H + \mathbf{n}^T \mathbf{C}_e \mathbf{n}} \tag{8}$$

where H is the hardening modulus, n is the flow rule vector that shows growth direction of the failure surface [11].

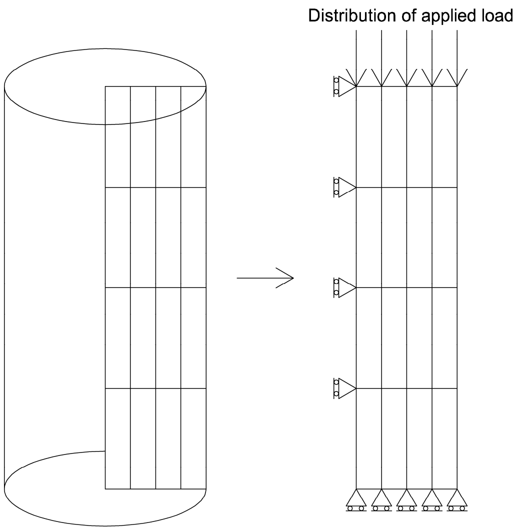

Fig. 2 The schematic configuration of generated mesh for axisymmetric cylinder

III. Results and Discussion

Farnam et al. [5] investigated the experimental responses of HSC, high performance fiber reinforced concrete (HPFRC), and slurry infiltrated fiber concrete (SIFCON) under compression with and without confining pressure. Four types of specimens with 0, 2, 5, 10% steel fibers volumes were tested by constructing 75 × 150 mm cylindrical specimens. The results of uniaxial tests are shown in Fig. 3; it can be seen that the plastic behavior and compressive strength increases as the steel fiber content increases. Moreover, enhancing fiber content has direct relation to the softening behavior of specimens. The more fiber content, the more dilation in the specimen behavior can be noticed. The advanced proposed model was implemented on the experiment results as illustrated in the aforementioned figure. As can be seen, the numerical response is in good accordance with the experimental data sets.

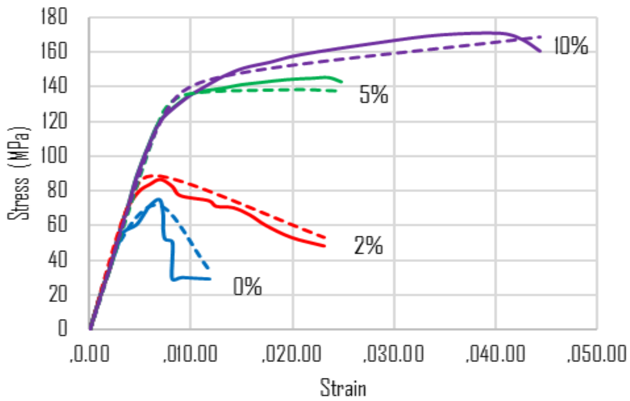

Fig. 3 Experimental and numerical stress-strain curves for HSC with various steel fiber ratios under uniaxial compression (solid and dashed lines stand for experimental and numerical results, respectively)

Noori et al. [6] studied the behavior of HPC and steel fiber-reinforced cementitious mortar (SFRCM). In order to assure the mechanical integrity upon initiation of cracks steel fibers were added to the mixture with 0, 1, and 2% content ratios. The experimental responses of the corresponding specimens have been depicted in Fig. 4. As can be seen, the numerical predicted behavior of aforementioned materials is in good agreement with experiments

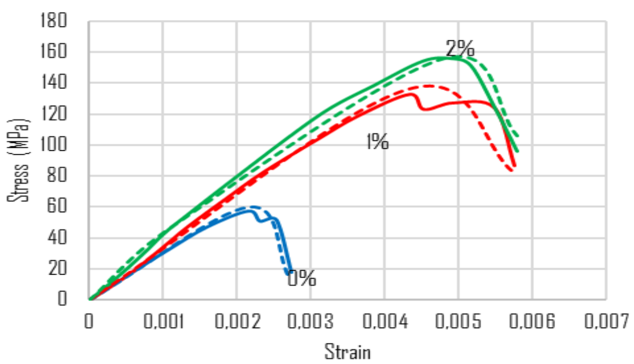

Fig. 4 Experimental and numerical stress-strain curves for HPC with various steel fiber ratios under uniaxial compression (solid and dashed lines stand for experimental and numerical results, respectively)

Toufigh et al. [7] investigated the behavior of PC with different epoxy resin ratios. The most important difference of PC with conventional types of concrete is that cement and water are substituted with epoxy resin, which improves the mechanical properties of material due to fast curing, durability and high strength. The outcome of experiments on PC with 12% epoxy resin ratio has been shown in Fig. 5. Accordingly, the numerical results for PC are also in great accordance with experiments.

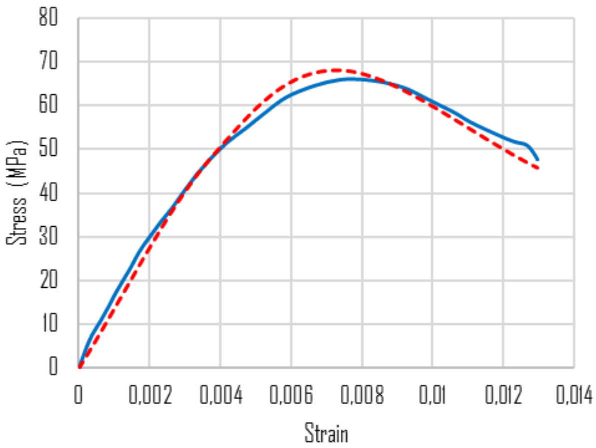

Fig. 5 Experimental and numerical stress-strain curves for PC with 12% epoxy resin ratio under uniaxial compression (solid and dashed lines stand for experimental and numerical results, respectively)

IV. Conclusion

In this paper, the stress-strain curves of 12% PC, HSC, and HPC with addition of steel fibers subjected to uniaxial compression loading were studied and modeled. Based on experimental results, PC showed superior properties including high compressive strength, excellent deformation, and fast curing. An advanced nonlinear model based on DSC and HISS failure criterion was proposed to predict the behavior of a wide range of materials. Since the model has more parameters than existing models, the numerical outcome was more accurately in agreement with experimental results including softening behavior.

References

[1] R. Bedi, R. Chandra, and S.P. Singh, “Mechanical properties of polymer Concrete,” *J. Compos.*, pp. 1–12, 2013.
[2] R. Bedi, R. Chandra, “Reviewing some properties of polymer concrete,” *The Indian Concrete Journal*, vol 88, no. 8, pp. 47-68, Aug. 2014.
[3] T.H. Wee, M.S. Chin, and M.A. Mansur, “Stress-strain relationship of high-strength concrete in compression,” *J. Mater. Civ. Eng.*, vol. 8 no. 2, pp. 70-76, May 1996.
[4] J.C. Lim, and T. Ozbakkaloglu, “Stress-strain model for normal- and light-weight concretes under uniaxial and Triaxial compression,” *Constr. Build. Mater.*, vol. 71, pp. 492-509, Nov. 2014.
[5] Y. Farnam, M. Moosavi, M. Shekarchi, S.K. Babanajad, and A. Bagherzadeh, “Behaviour of slurry infiltrated fibre concrete (SIFCON) under triaxial compression,” *Cement Concrete Res.*, vol. 40, no. 11, pp. 1571-1581, Nov. 2010.
[6] A. Noori, M. Shekarchi, M. Moradian, and M. Moosavi, “Behavior of Steel Fiber-Reinforced Cementitious Mortar and High-Performance Concrete in Triaxial Loading,” *ACI Mater. J.*, vol. 112, no.1, pp. 95-104, Jan.-Feb. 2015.
[7] V. Toufigh, M. Hosseinali, and S.M. Shirkhorshidi, “Experimental study and constitutive modeling of polymer concrete’s behavior in compression,” *Constr. Build. Mater.*, vol. 112, pp. 183-190, Jun. 2016.
[8] C.S. Desai, *Mechanics of materials and interfaces: The disturbed state concept*. CRC press, 2000.
[9] C.S. Desai, "Constitutive modeling of materials and contacts using the disturbed state concept: Part 1 – background and analysis," *Comput. Struct.*, vol. 146, pp. 214-233, Jan. 2015.
[10] A. Khoei, *Computational plasticity in powder forming processes*. Elsevier, 2010.
[11] A.H. Akhaveissy, C.S. Desai, S.A.A.D. Sadrnejad,; and H. Shakib, "Implementation and comparison of a generalized plasticity and disturbed state concept for the load-deformation behavior of foundations," *Sci. Iran.*, vol. 16, no. 3, pp. 189-198, May-Jun. 2009.